Accepted manuscript doi:
10.1680/jgeen.21.00104

Submitted: 04 June 2021

Published online in 'accepted manuscript' format: 13 August 2021

Manuscript title: Assessing single helix screw pile geometry on offshore installation and axial capacity

Authors: Yaseen Umar Sharif[1], Michael John Brown[1], Matteo Oryem Ciantia[1], Benjamin Cerfontaine[2], Craig Davidson[1], Jonathan Adam Knappett[1] and Jonathan David Ball[3]

Affiliations: [1]School of Science and Engineering, University of Dundee, Dundee, UK; [2]Engineering and Physical Sciences, University of Southampton, Southampton, UK and [3]Roger Bullivant Ltd, Burton Upon Trent, UK

Corresponding author: Yaseen Umar Sharif, School of Science and Engineering, University of Dundee, Fulton Building, Dundee, DD1 4HN, UK.

E-mail: y.u.sharif@dundee.ac.uk

This research was funded in whole, or in part, by the Engineering and Physical Sciences Research Council (Grant no. EP/N006054/1. For the purpose of open access, the author has applied a CC BY public copyright licence to any Author Accepted Manuscript version arising from this submission.

Accepted manuscript doi:
10.1680/jgeen.21.00104

Abstract

Due to their low-noise installation and relatively large axial capacity, screw piles have been proposed as an alternative foundation solution in dense sand for offshore renewable energy applications in deeper water. For this to occur, a significant upscaling of onshore dimensions is required. Furthermore, the effects of certain geometric features on installation requirements are still not well understood. In this paper, the effects of base geometry, shaft diameter and helix pitch were investigated using the three-dimensional discrete-element method by simulating the full installation process prior to conducting axial compression and tension tests. The results of the investigation showed it is possible to optimise the geometry of the screw pile to reduce installation requirements, in terms of both vertical installation force (up to 61%) and installation torque (up to 39%), without reducing the axial capacity of the pile significantly.

Keywords: geotechnical engineering; piles & piling; computational mechanics

Accepted manuscript doi:
10.1680/jgeen.21.00104

1 Introduction

Screw piles are steel displacement piles that consist of a straight shaft or core with one or more helices welded to the core at regular intervals (Lutenegger, 2011) (Figure 1). Onshore screw piles are typically installed by applying a torque with the additional of vertical compressive (crowd) force to the top of the pile using a torque head attached to an excavator (DFI, 2019; Richards *et al.*, 2019). Currently onshore screw piles are used to anchor light structures such as telecommunication towers (Schiavon *et al.*, 2016), and as foundations for buildings (Lutenegger, 2013), small onshore wind turbines, and bridges (Livneh and El Naggar, 2008). Historically screw piles have been used as offshore foundations to support near shore structures, such as lighthouses and piers (Lutenegger, 2011). It has been proposed that screw piles could be used as an alternative solution for offshore renewable energy deployment in deeper water (water depths up to 80m) (e.g. Davidson *et al.*, 2020), due to their ease of installation and the "silent" installation. For this to occur significant upscaling of existing onshore screw pile geometries is required, which raises concerns over the practical challenge of installing large diameter screw piles in the offshore environment where very large reaction forces may not be readily available from installation vessels.

$$AR = \frac{\Delta z_h}{P_h} \qquad (1)$$

Davidson *et al.* (2020) have shown, through centrifuge modelling, that screw pile geometries capable of supporting a typical four-legged jacket structure would require significant installation requirements (installation torque 7 MNm and compressive installation forces 23 MN) when installed under pitched-matched conditions. This suggests there is a need to investigate how installation requirements can be reduced to further develop their use offshore. Sharif *et al.* (2020b) have shown that by reducing the advancement ratio (AR), the ratio between the vertical displacement for one rotation (Δz_h) over the helix pitch (P_h), below 1 (where 1 represents pitch-matched installation; Equation 1), it was possible to reduce the compressive installation forces of screw piles significantly and even install a screw pile under its own "self-weight", although this had little effect on the installation torque which remained substantial.

It was also found that AR influences the in-service or post-installation performance of the screw pile, with $AR < 0.8$ (over-flighting) improving the tensile performance but decreasing the compressive performance and $AR > 0.8$ having the reverse effect (Sharif et al. 2020b). The increase in tensile capacity for screw pile installed at $AR < 0.8$ is due to the particles being transported through the helix and compressed above it during the installation process, resulting in a denser soil and a high stress region being present above the helix post installation. In contrast to this, for screw piles installed at $AR > 0.8$ the particles below the helix experience a similar mechanism to that of a bearing capacity failure and are displaced below and around the helix, generating a large residual stress below the helix and a low stress region above the helix at the end of installation. Thus, giving the $AR < 0.8$ screw piles a higher compressive performance. This phenomenon is currently only known to occur in sand, with the effects of AR not fully investigated in other soil types. These effects have been observed though both the Discrete Element Method (*DEM)* (Sharif et al. 2020b) and scale model centrifuge testing (Cerfontaine *et al.*, 2021).

One possible way to reduce the installation torque and potentially further optimise the installation force is to change the geometric features of the screw piles, such as the base geometry, shaft diameter and helix pitch. A study on rotary installed straight shafted piles by Sharif *et al.* (2020a) through *DEM* has shown that changing the base geometry of a solid pile from a flat base to a 40° conical tip, reduces the base component of installation force by up to

Accepted manuscript doi:
10.1680/jgeen.21.00104

68% and the base component of the installation torque by up to 80% in dense sand (although it should be noted that installation torque was primarily generated by the shaft of the pile in this study). 1g laboratory tests conducted in dense sand by Saleem *et al.* (2020) on the installation and axial performance of screw piles installed pitch-matched (AR = 1.0) with different base geometries, also indicated that modifying the base geometry can impact the installation requirements. Screw piles with varying base geometry (flat, conical tip with an apex angle of 90°) were installed with a conical base reducing the installation torque by 14% and installation force by 19% when compared to the flat base. The base geometry also influenced the post-installation compressive capacity of the installed pile, with the conical tip reducing the compressive capacity measured at a displacement of 0.1 D_h by 12.5%. This highlights the need to consider both installation requirements and in-service performance when designing a screw pile for offshore use.

In offshore applications, the foundation would be required to resist large forces, both axially and horizontally, due to wave, wind and current loading. Davidson *et al.* (2020) have suggested that for a large jacket structures supporting an offshore wind turbine installed in a water depth of 80 m, an individual pile installed at one corner could be required to endure a compressive force of 35MN, a tensile load of 26MN and a lateral load of 6MN. This results in not only an increase in the size of the screw pile, compared to their onshore counterparts, but also specific geometric properties would need to be modified, such as an increased shaft diameter in order to resist the large horizontal loads (Al-Baghdadi *et al.*, 2017; Davidson *et al.*, 2019). The increase in shaft diameter would result in a large surface area associated with the shaft of the screw pile, but also an increase in the area of the base. From the centrifuge and *DEM* findings on rotary installed straight shafted piles by Sharif *et al.* (2020a) and Deeks (2008), it is known that installation torque for straight shafted piles is primarily generated by the shaft of the pile and the installation force by the base. Therefore, a potential method to reduce the installation torque is to reduce the shaft diameter, although as previously noted this dimension is primarily controlled by the required lateral capacity and bending moment resistance of the upper sections of the pile. Screw pile designs such as those of Davidson *et al.* (2019) and dos Santos Filho *et al.* (2014) attempt to combat the issue of reduced lateral capacity by using an optimised screw pile core. These designs have a smaller shaft diameter for the lead section of the pile (to reduce the installation torque) and a larger shaft diameter close to the surface to provide the required structural capacity, where lateral effects are generally limited to the upper sections of a long pile.

Another geometric feature which could influence the installation requirements of the screw pile, is the geometric pitch (P_h) (Figure 1). The geometric pitch for onshore geometries is rarely varied and is typically set at 3 inches (76 mm) as recommended by Perko (2009) and International Code Council (2017). In a field study, Lutenegger (2013) installed three screw piles with the same shaft and helix diameter (D_h = 0.3 m to an installation depth of 3.0 m) but with varying pitch, (3, 4 and 6 inches or 76.2, 101.6 and 152.4 mm) with subsequent tensile tests on the installed screw piles. These tests suggested that the pitch had an effect on the installation torque (increase of 50% by increasing P_h from 76 mm to 152.4 mm). The vertical force during installation was not recorded, as is usually the case in field studies and therefore it is unknown how this was affected. No discernible effect of pitch was observed in the tensile capacity results, which may suggest no significant influence or could be attributed to the variability of testing in the field.

Accepted manuscript doi:
10.1680/jgeen.21.00104

An additional motivation for this study was to investigate the effect of geometric changes on the empirical relationship between torque and axial capacity that is widely used in practice. It is often suggested that the torque (T) required to install a screw pile can be directly correlated to its ultimate capacity (Q_T or Q_C) through a unique factor (K_t or K_c for tension and compression respectively; Equation 2) which is selected based upon the shaft diameter (D_s) (Equation 3) (Hoyt and Clemence, 1989; Perko, 2009; Tsuha and Aoki, 2010).

(2)

where Q_t is the axial tensile capacity of a screw pile and T is the installation torque at the end of installation. Perko (2009) related the K_t factor to the diameter of the pile shaft (D_s) by fitting the following equation to field and model experiments:

(3)

where D_s and K_t have units of m and m^{-1} respectively. Perko (2009) also suggested that a single factor could be used to predict both tensile and compressive capacities. However, the data set used by Perko (2009) contains considerable scatter using a limited number of shaft diameters, which were far below those which may be used for offshore deployment (Davidson *et al.* 2020). Lutenegger (2013) suggests that it may be incorrect to assume that a single parameter model is effective for all screw pile geometries as is suggested by Equation 2&3, as it does not consider the effect of any geometric property other than the shaft diameter, nor any influence of pile depth (H/D_h) or soil properties (Davidson *et al.* 2020, Sharif *et al.* 2020b).

Sakr (2015) further developed the values of K_t for screw piles with larger shaft and helix diameters. Rather than using a single K_t value based upon the shaft diameter of the screw pile, Sakr (2015) used the installation torque prediction method first introduced by Ghaly and Hanna (1991) and the axial capacity prediction method proposed by Das (1990) to calculate a K_t value. Both prediction methods use soil properties and additional geometric features (such as helix diameter and pitch) to calculate their respective values. Although, some geometric and installation parameters are not included, such as advancement ratio and base geometry.

This paper investigates the effect of screw pile geometry on the installation requirements and in-service axial performance of a screw pile using *DEM*. Twelve simulations were conducted, varying the advancement ratio and screw pile geometry (base shape, shaft diameter and helix pitch). An additional simulation was also conducted in which a straight shaft pile of the same core diameter was installed into the dense soil bed for comparison purposes. The results show that it is possible to optimise the installation requirements of a screw pile (reducing the installation force and torque), without significantly affecting the in-service axial performance.

1 Methodology

The Discrete Element Method (*DEM*) is a numerical modelling framework which can be used to model large deformation problems in granular soils (Ciantia *et al.*, 2019). Unlike continuum modelling such as the Finite Element Method (*FEM*), *DEM* uses discrete particles that are able to interact to model the behaviour of a soil body. *DEM* has previously been used to model a variety of different soil structure interaction problems such as pile plugging (Liu *et al.*, 2019), cone penetration tests (Butlanska *et al.*, 2014), slope stability (Kim *et al.*, 1997) and jacked piles in sand (Ciantia *et al.*, 2019) including their cyclic response after installation (Ciantia, 2021). Through calibration and validation of the contact models (against triaxial tests or centrifuge model tests), the particle assembly is able to mimic the behaviour of a

Accepted manuscript doi:
10.1680/jgeen.21.00104

granular soil bed, with the added benefit of using a single or the same particle assembly multiple times by resetting it to its original condition (Shi *et al.*, 2019).

Particle Flow Code 3D 5.0.35 (Itasca Consulting Group, 2016) was used. The interaction between the individual particles and between the particles and structure were modelled using a simplified Hertz-Mindlin contact model (Mindlin and Deresiewicz, 1953). Spherical particles were used, with the rotation of the particles inhibited to capture the rotational resistance of angular grains (Arroyo *et al.*, 2011; Ciantia *et al.*, 2019). Viscous damping was not used in either of the contact models and critical damping was set to 0 as the simulation occurred under quasi-static conditions. The maximum vertical velocity used within the *DEM* simulations was 0.5 m/s at the full installation depth and was calculated using the equations outlined in Sharif *et al.* (2020b) ensuring that the simulation remained quasi static. The centrifuge tests of Davidson *et al.* (2020) were conducted at 3rpm and 21 mm/min, such that both the centrifuge and DEM tests are conducted under drained soil conditions.

The parameters for the particle-particle and particle-structure contact models were calibrated against loose and dense laboratory triaxial tests and geotechnical centrifuge experiments of rotary installed and axially press in straight shafted piles respectively (Sharif *et al.*, 2019a), and were validated against further centrifuge experiments of screw piles (Sharif *et al.*, 2019b; Davidson *et al.* 2020; Cerfontaine *et al.*, 2021). Additional details on the calibration and validation of the contact models can be found in Sharif *et al.* (2019a, 2019b). The sand modelled in the *DEM* is based upon the properties of HST95 which is a medium to fine well-graded sand that is commonly used at the University of Dundee (*UoD*) in physical modelling (Davidson *et al.*, 2020) and element testing (Robinson *et al.*, 2019). The behaviour and properties of the soil have been previously investigated and are well documented (Al-Defae *et al.*, 2013; Lauder *et al.*, 2013). The *DEM* parameters for the contact models are shown in in Table 1.

1.1 Sand bed preparation

The *DEM* particle assembly was created in accordance with the specification outlined in Sharif *et al.* (2019b). This methodology uses the periodic cell replication method (Ciantia *et al.*, 2018) and the particle refinement method (McDowell *et al.*, 2012) to create soil beds with a homogeneous voids ratio and a linear increase in effective stress with depth. To generate the sol bed, a thin slice of particles (3.5 D_{100} thick) is initially generated using the radial expansion method and is compressed to the target voids ratio and maximum effective stress of the soil bed. The slice is then replicated vertically to the desired height of the final soil bed and the contact forces between particles are then scaled to achieve a linear increase in effective stress with depth. A detailed description of the soil bed formation process can be found in Sharif *et al.* (2019b). An example soil bed can be seen in Figure 2a, with the voids ratio of the soil bed outlined in Figure 2b. To model the effective stress within a saturated soil bed using a dry soil bed the approach developed by Li *et al.*, (2010) for centrifuge modelling was adopted. This methodology uses a lower gravitational acceleration on a dry soil bed such that the effective stress of the dry soil bed mimics the effective stress state of a saturated soil bed. Thus, the simulations represent screw piles installed into a saturated normally consolidated sand under drained conditions. This methodology has previously been used in centrifuge modelling by Davidson *et al.*, (2020) and *DEM* modelling by Sharif *et al.* (2020b) to model the drained installation and axial capacity of large diameter piles in sand.

The prototype dimensions and properties of a dense sand bed (D_R = 84%) can be seen in Table 2. Dense sand was chosen as this would produce the largest resistance to installation and therefore would provide an upper bound of what is likely to occur during offshore deployment. To avoid any boundary effects, the radius of the soil bed was chosen to be

Accepted manuscript doi:
10.1680/jgeen.21.00104

greater than the 20*R* suggested by Bolton *et al.* (1999), where *R* is the radius of the pile helix (i.e. the largest radius of the pile), which has been shown by (Sharif, *et al.*, 2020a) to be sufficient in *DEM* modelling of penetration problems. Sharif *et al.* (2020) showed that no increase in effective stress was recorded 13*R* from the centre of the soil bed when installing a straight shafted pile.

To reduce the run-time of the simulations, a particle size distribution (*PSD*) scaling value (*N*) of 20 was used in the centre of the soil bed, with a maximum *N* equal to 96.5 used at the boundary. This value represents the multiplier applied to the particles' diameter, so that each DEM particle represents N^3 soil particles, with the bulk properties of the soil remaining the same. The particle scaling of 20 was selected based upon the recommended ratio of pile core diameter (D_s) to the median particle size (d_{50}), in the core of the soil bed, of 2.69 (Arroyo *et al.*, 2011). The size of the helix pitch (P_h) must also be sufficiently large to avoid causing a blockage of particles in the helix opening. In this series of simulations the minimum ratio of P_h to the maximum particle size in the central core (d_{100}) was 2.65, as in Sharif *et al.* (2020b). This typically results in at least 15 to 17 particles passing through the smallest helix opening at any given time, eliminating the possibility of a blockage occurring. The increase in particle scaling in the central core, increases the level of "noise" that appears in the data, although from Sharif *et al* (2019a) it can be seen that the results are able to accurately match those of physical centrifuge tests.

1.2 Pile models

The base or reference geometry of the screw piles used in study is that of the U1VDB pile used in the centrifuge modelling of Davidson *et al.* (2020) (Figure 1). The screw pile consists of a single helix diameter (D_h) of 1.70 m and a helix pitch (P_h) of 0.56 m with a flat artificially plugged base and a shaft diameter (D_s) of 0.88 m (Figure 1). The thickness of the helix was 1.3 mm. The screw pile has an embedment depth to the helix (*H*) of 12.3 m resulting in a relative embedment depth (H/D_h) of 7.2. This base pile geometry was then modified with each variant changing only one aspect of the base U1VDB pile geometry (Table 3). The geometric features that were modified include the base, the shaft diameter and the helix pitch. The diameter of the helix remained constant to ensure that direct comparisons of the screw piles' axial capacity could be made at the same installation depth. All piles were modelled to have no self-weight or mass, as it assumed that the mass of the displaced soil is equal to that of the installed pile. The screw piles were segmented into component parts (base, helix, shaft), with each segment consisting of a rigid boundary which move in unison with one another. This allows for directional force readings to be recorded from each segment during the simulation, in effect creating a fully instrumented pile which would be difficult to achieve in scaled physical model testing.

The modifications to the base geometry consist of a cone with an apex angle of 40° and an asymmetric cut-off with a 45° inclination (see Figure 1). The apex angle of the conical tip was chosen based on the recommendations for reducing installation requirements of rotary installed straight shafted piles by Sharif *et. al* (2020a). The asymmetric cut-off is a base geometry commonly seen in onshore screw piles (Elsherbiny and El Naggar, 2013) and is typically used to 'stab' the pile into the ground for stability during the initial penetration. However, it is unclear from existing literature what effect this geometry has on the installation requirements and the in-service capacity of the screw pile. All piles were modelled as artificially plugged (solid core), as was the case in the centrifuge tests of Davidson *et al.* (2020), to model the worst-case plugged scenario during the installation process. This gives the upper bound resistance for the installation requirements. Two additional shaft diameters were considered, 1.20 m and 0.60 m, resulting in D_s/D_h = 0.35,

Accepted manuscript doi:
10.1680/jgeen.21.00104

0.51 and 0.71. The final geometric change was a pile with an increased helix pitch (P_h) of 1.20 m. Due to particle size constraints it was not possible to test a smaller helix pitch, as particles would be unable to easily pass through the helix opening.

1.3 Modelling procedure

For each simulation the screw pile was installed into the soil bed at two advancement ratios (Equation 1). According to the recommendation of BS8004 (2015) and Perko (2008) a screw pile should be installed at an advancement ratio of 1.0 to avoid the effects of "disturbance" to the soil during installation which would significantly reduce the in-service performance. From the work of Sharif *et al.* (2020b) it was shown that the installing at advancement ratios other than 1.0 does not necessarily reduce the in-service performance implied by "disturbance" but that the *AR* can be optimised to increase performance in either tensile or compressive loading. Sharif *et al.* (2020b) showed that for $AR > 0.8$ the compressive performance can be increased and for $AR < 0.8$ the tensile performance is increased. In this study all piles were installed at both $AR = 1.0$ and 0.5.

Once the screw pile had been installed to the desired depth the piles were then unloaded and constant rate of penetration tests (*CRP)* were conducted to obtain the compressive and tensile capacity of the installed pile, with the model being reset to its unloaded state between axial capacity tests. During the *CRP* tests the pile was restricted from rotating and was only displaced axially.

2 Results and discussion

Figure 3 shows the total installation force and torque (recorded at the head of the pile) of all pile geometries used within this study. From figure 3a and figure 3c it can be seen that the most effective method for reducing the installation force is by over-flighting the screw pile as suggested by Sharif *et al.* (2020) although this method does not decrease the installation torque significantly (Figure 3b and 3d). Figure 3b and 3d show torque is reduced by decreasing the shaft diameter of the pile. The screw pile with a shaft diameter of 0.60m shows a decrease in installation torque of 32% when pitch-matched and 34% when over-flighted when compared to the flat base pile (D_s = 0.88m) installed at the same *AR*.

As the screw piles have been split into component parts, it is possible to determine the contribution of each of the geometric features to the installation requirements. Figure 4a, shows that for the base case pile (flat base, P_h = 0.56 m and D_s = 0.80 m) the largest contributor to the installation force was the base of the screw pile (82.1%) with the helix contributing 17.2% and the shaft with the lowest contribution at 0.7% for the pitch-matched installation. When looking at the installation torque for the same pile (Figure 4b), the helix contributed the largest portion (71.3%), followed by the base component (21.3%) and the shaft component contributed only 7.6% of the total installation torque.

For the over-flighted screw pile (AR=0.5) the distribution of installation force was drastically different (Figure 4a), with the helix of the screw pile recording no significant vertical resistance to penetration, the base resistance remaining unchanged from that of the pitched match installation and the shaft component also remaining negligible. Installation torque also appeared to be unchanged (Figure 4b).

From this it can be determined that in order to further optimise the installation force, the base component must be reduced as this remains the highest contributor when over-flighting. This could be achieved by either changing the shaft diameter or the geometry of the base itself. In terms of the installation torque the helix component remained dominant for both installation methods and therefore would be the targeted area of investigation for optimising the installation torque.

Accepted manuscript doi:
10.1680/jgeen.21.00104

The axial capacity of the piles was defined as the resistance at a pile displacement equivalent to $0.1D_h$. In compressive capacity prediction methods, the contribution base of the pile to compressive capacity is incorporated into the helix component, and the full diameter of the helix is used to calculate its cross-sectional area. In this study, the contribution of the base and the helix to the compressive capacity have been considered independently (as the base geometry has been varied), and as such the helix component of axial resistance only represents the resistance produced by the net area of the helix. In tension the base plays no part in the resistance and only the net area of the helix contributes to the load capacity. The breakdown of the axial capacity into component parts can be seen in Figure 4c and 4d. Figure 4c shows that early stiffness of the compressive load displacement curve was generated by the base of the pile before the helix was able to fully engage at a normalised displacement of 0.006 (vertical displacement /helix diameter, z/D_h) . The shaft did not contribute to the compressive capacity as would be expected due to it being shielded by the helix. This can be seen in the reduction of the shaft resistance between the U1VDB screw pile and the straight shafted pile in Figure 4c. Figure 4d shows the breakdown of the axial tensile capacity. The base of the pile played no part in the tensile resistance. The helix produced the most resistance (90%) and the shaft contributed the remaining 10% at $z/D_h = 0.1$. This is in line with the results of Urabe *et al.* (2015) who also showed a shaft contribution of between 5.9 to 10.8% of the total tensile capacity of their screw pile installed in dense sand. Once again, the shaft resistance has been reduced when compared with the straight shafted pile, although the inclusion of the helix has greatly increased the total tensile performance. The distribution of the loads during the axial *CRP* tests are indicative of screw piles installed to relatively shallow embedment depths ($H/D_H < 9$), screw piles installed to greater embedment depths may show an increase in the shaft resistance contribution.

Table 4 shows the empirical torque capacity factor calculated from the simulations conducted in this investigation in both tension and compression (K_T and K_C respectively). The back calculated K values vary considerably in both tension (1.14 m^{-1}-2.53 m^{-1}) and compression (2.19 m^{-1}-7.14 m^{-1}) with only a single value being close to the K factor (2.6 m^{-1}) calculated using Equation 3 for the 0.88 m shaft diameter pile. The K_T and K_C values are also lower than those predicted using the Sakr (2015) method (K_T = 7.6 m^{-1} – 10.36 m^{-1} and K_c = 7.5 m^{-1} – 12.15 m^{-1}), mainly due to the overprediction of axial capacity when using the Das (1990) compression and tensile capacity prediction methods. No discernible trend can be seen when comparing the K factors for the piles with varying shaft diameter. Therefore, it seems that piles with the same shaft diameter, but varying helix and base geometries do not have the same torque correlation factor (especially when considering K_c), which contradicts the implicit assumption of Equation (3). It is also prudent to state that for large screw pile diameters with relatively short embedment depths (H/D), Equation (3) should be used with caution and different K factors should be considered in tension and compression.

2.1 Effect of Base geometry

Figure 5 shows the base component installation force and torque for the screw piles with varying base geometry. Figure 5a shows that by modifying the base of the pile from a flat tip to an asymmetric cut off it was possible to reduce the base component of the installation force by up to 50%. A base cone with apex angle of 40° results in a 50% reduction in base component of installation when installing the screw pile under pitch-matched conditions compared to that of the flat base. The contribution of the helix and shaft to the total installation force remained the same for all three base geometries.

Accepted manuscript doi:
10.1680/jgeen.21.00104

When assessing the base component of installation torque (Figure 5b), the asymmetric cut off resulted in a significant increase compared to the flat base pile, with the shaft and helix contribution decreasing by a small amount, resulting in the asymmetric cut off pile having a slightly higher total torque than that of the flat base pile for both *AR* values. The increase in torque is due to the larger surface area of the asymmetric cut off tip (240% increase in surface area) where it is assumed that all piles are plugged. Of the three base geometries that have been investigated the conical tip has the lowest contribution to the installation torque, with a small increase in the helix contribution. As a result of this the screw pile with the conical tip has the lowest installation torque of the three base geometries, although only by a small margin. This is in agreement with the study of Sharif *et al.* (2020a), who found the optimum apex angle for the conical base was 40° and Saleem *et al.* (2020) who also showed that a conical base (with apex angle 90°) reduced both the installation force and torque for rotary installed piles compared to a pile with a flat tip.

For the over-flighted screw pile, the reduction in base component of vertical force followed the same pattern as that of the pitched-matched installation (Figure 5a), i.e. the flat base has the highest compressive force and the conical base the lowest with only small reductions occurring due to the increase in rotation rate as discussed by Sharif *et al.* (2020a). Installation torque remained predominantly the same as that of the pitched-matched installation (Figure 5b). Therefore, for both advancement ratios the most appropriate base geometry for a solid pile is the 40° conical tip, as it was able to reduce the compressive installation force whilst also resulting in a 5% reduction in installation torque.

When assessing the in-service compressive performance of the piles, it can be seen (Figure 6a) that the flat base had the highest compressive capacity (31MN) and the asymmetric cut off the lowest (26MN), with the cone only slightly higher (27MN). The lower compressive capacity is to be expected as both the asymmetric and the conical base had a lower resistance during the installation phase. This result is also in agreement with that of Tovar-Valencia *et al.* (2021) who showed that a conical tipped jacked straight-shafted pile will have a lower compressive capacity than one with a flat base. In terms of the tensile capacity of the pile, there is no measurable variation between the piles with the different base geometries (Figure 6b). This is due to the base playing no part in the tensile capacity, as the helix provides 90% of the resistance and the shaft 10%. As the tensile capacity may be the critical factor for axial performance of screw piles installed in the offshore environment (depending on application), the reduction in compressive base resistance is not significant.

From these results, in order to further optimise the installation requirements of the screw pile, the best base geometry is the 40° conical tip, as it provides a large reduction in installation force, with no increase in installation torque. The conical tip also has no significant effect on the in-service performance of the screw pile (if tensile performance is the governing factor) and therefore is not detrimental to its application.

2.2 Effect of Helix Pitch

The two helix pitches tested within this study showed exactly the same installation requirements when installed in a pitched-matched manner, with no differences being observed in either the installation force or torque (Figure 3a and 3b). For the over-flighted screw piles (*AR* =0.5) (Figure 3c), the P_h of 1.20m had a total installation force 68% lower than that of the 0.56 m helix pitch screw pile. The helix contribution to the installation force for the over-flighted screw piles showed that the 1.20 m helix pitch was able to provide additional pull-in force whereas the 0.56 m helix pitch had a negligible compressive vertical force or resistance to penetration acting upon it (Figure 7a). The tensile force seen for the larger helical pitch means that the vertical force on the lower surface of the helix is smaller

than that of the reaction force on the upper surface of the helix (i.e. a reduction in stress below the helix and an increase in stress above as material passes through the helix opening during over-flighting). This is potentially due to the larger helix opening being able to move much more material through the helix, in a single rotation, and compacting it above as the helix advances, reducing the vertical stress below the helix and increasing it above. The potential increase in vertical stress and the larger surface area would result in a tensile pull in force from the helix as seen in Figure 7a.

Figure 7b shows the final helix component of the installation torque reduced by approximately a third when helix pitch was increased. As the total torque (Figure 3b and 3d) was unchanged a redistribution occurred, and the shaft component for P_h = 1.20 m increased for both advancement ratios. The increase in the shaft component of torque is a result of the increase in shaft surface area located within the helix opening, which is known to be a location of high radial stress (Sharif *et al.* 2020b) during installation. Therefore, decreasing the surface area of the shaft within this region (decreasing the shaft diameter) would result in a reduction of the installation torque and optimisation of installation requirements.

When assessing the compressive and tensile capacity, it can be seen that there is a significant difference between the performance for P_h of 1.20 m compared to 0.56 m for both installation methods (Figure 8). The larger helix opening showed better performance in tension (Figure 8a) whereas P_h = 0.56 m showed a better performance in compression (Figure 8b) when installed at AR =1.0. The compressive capacity for P_h = 1.20 m was ultimately able to match that of P_h = 0.56 m but large displacement was required for this to occur ($0.2D_h$). By extracting inter-particle contact forces at the end of installation (as was conducted by and O'Sullivan *et al.* (2010); Ciantia *et al.* (2019); Sharif *et al,* (2020)) it was possible to investigate the distribution of the residual vertical stresses (σ_{zz}) within the soil caused by the introduction of the pile (Figure 9a). Figure 9a shows the vertical stress surrounding the piles installed at AR = 1.0, as this is the installation method which had the largest difference in performance between the two piles. For P_h = 1.20 m a large region of high stress was present above the helix, which was not present in the 0.56 m pitch case, which has a larger region of stress below the helix. The high stress region above the helix would result in a stiffer tensile performance as seen in Figure 8b for P_h = 1.20 m, whereas a larger stress region below the helix would result in an increase in compressive stiffness as seen in Figure 8a for the 0.56 m helix pitch. The change in vertical position of particles (δz) from the start to the end of the installation process (Figure 9b) shows that the smaller helix pitch displaced much more soil downwards during its advancement, creating a larger bearing capacity failure below the base and helix of the pile, than that of the larger helix pitch. This in turn resulted in the larger region of stress below the base and helix as indicated in Figure 9b.

As only two helix pitches were simulated in this study, further investigation into this is required using both smaller and larger helical pitches and smaller particles (to accommodate the smaller helical pitches).

2.3 Effect of Shaft diameter

When assessing the influence of the shaft diameter on the installation requirements of the screw pile it is important to investigate all components of the pile, as an increase in the shaft diameter will also increase the surface area of the base of the pile and thus reduce the surface area of the helix (where the outer diameter is kept constant for comparison). For pitch-matched installation, it can be seen (Figure 3a and 3b) that there is an increase in both installation force and torque as the shaft diameter increases, although the biggest increase is from D_s = 0.60 m to D_s = 0.88 m (61%) with a much smaller increase from D_s = 0.88 m to D_s =1.20 m (29%).

Accepted manuscript doi:
10.1680/jgeen.21.00104

This increase in both installation requirements was primarily due to the larger surface area of the pile base and not that of the shaft itself (Table 5). As previously mentioned, the shaft of the pile contributed very little to the total installation requirements (Figure 4). The results also indicated a redistribution of the installation force and torque between the helix and the base (Table 5) when altering the shaft diameter, with D_s = 1.20 m resulting in the base having a larger contribution than the helix in terms of installation torque. Reducing the shaft diameter results in significant reductions in the base component, as expected, with the helix contributing the highest proportion of vertical compressive force.

For the over-flighted screw piles, the installation force of the two larger shaft diameters remained in compression while the installation force of the smallest shaft diameter was close to 0MN (Figure 3c). This is due to the large reduction in base resistance as well as a pull in force from the helix due to its larger surface area and the reduction in displacement of particles as a much smaller volume was needed to accommodate the shaft of the screw pile. No significant change was seen in the installation torque between the two advancement ratios (Figure 3b and 3d).

Figure 10a shows that as the shaft diameter increased the compressive capacity remained the same, whereas in Figure 9b the tensile capacity increased with an increase in shaft diameter. This difference can be explained by investigating the change in relative density (between initial and post-installation soil state (ΔD_R)) of the soil surrounding the pile (Figure 11a), in addition to the soil stress state post installation (Figure 11b) for the pitch-matched installation (AR = 1.0). From Figure 11a it can be seen that there was a reduction in relative density surrounding all three screw pile geometries. The smallest shaft diameter (D_s = 0.60 m) showed the largest reduction in relative density and the largest shaft diameter (D_s = 1.20 m) had the smallest reduction in relative density close to the pile shaft (up to $0.5D_h$ from the centre of the pile). The difference in tensile stiffness can be explained by the location and strength of the residual vertical stresses within the soil post installation. Figure 11b shows that the region of high stress above the helix increases in size and magnitude with the shaft diameter (D_s = 0.60 m ≈ 400kPa, D_s = 1.20 m ≈ 700kPa at a depth of 10m below ground level (BGL)). As the screw pile is installed, soil must be displaced to accommodate the volume of the advancing pile. The smaller the pile is, the less displacement is required, resulting in lower stresses being induced within the surrounding soil and therefore lower residual stresses once it has been unloaded. This would result in the smallest shaft diameter having the lowest ultimate tensile capacity and the largest shaft diameter the highest ultimate tensile capacity (defined at $0.1D_h$ of vertical displacement).

In contrast to this in both Figure 11a and 11b the soil condition below the helix appeared to be relatively unchanged when comparing the different shaft diameters and as a result the compressive response remained similar, despite the shaft diameter varying (Figure 10a).

From this data it is possible to surmise that the optimum method for reducing the installation torque of a screw pile is to have as small a shaft diameter as possible. However, this method may not be possible for screw piles designed for the offshore environment, due to the large reduction in tensile capacity it results in and the need for significant structural capacity to resist the large bending moments produced by lateral loads in-service. A potential, solution would be to use piles with “optimised” shafts, which would have a smaller shaft diameter for the lead section of the pile (close to the base of the pile and helix) and larger shaft diameter for the upper portion of the pile (at the head of the pile) such as the O2VD pile from Davidson *et al,* (2020) or the A1/A2 pile geometries used by dos Santos Filho *et al.* (2014). The reduced lead section would reduce the base component of the installation requirements, while the upper section would be able to resist the large lateral loads.

3 Conclusion

In this paper the effect of screw pile geometry on the installation requirements and in-service axial performance of screw piles was investigated using the discrete element method. An existing screw pile fulfilling the requirements of an offshore jacket foundation was modified to find its optimal geometric configuration. Each pile was installed into a simulated dense sand bed at advancement ratios of 1.0 (pitched-matched) and 0.5 (over-flighted) before conducting an axial constant rate of penetration tests in compression and tension.
The investigation has highlighted the following findings:

- Modifying the geometry of the base of the pile can significantly reduce the required compressive installation force by upto 50%, this has no impact on tensile performance but decreases the compressive capacity by a small amount.
- Varying the helix pitch has no impact on the installation requirements when installing under pitch matched conditions but decreases the required installation force when over flighting ($AR = 0.5$).
- The size of the helix pitch does appear to affect the axial capacity of the screw pile, with the large helix pitch showing an increased tensile performance and the smaller helix pitch having an increased compressive capacity. Suggesting the helix pitch can be optimised based upon its in-service requirements.
- The shaft diameter was shown to be the most effective method for decreasing the installation requirements, with a 61% reduction in installation force, although this has been shown to also reduce the tensile resistance by 42%.
- A reduction in section size would also likely to result in a reduced structural strength, limiting its ability to resist the large bending moments associated with wind and wave loading on offshore renewable structures. A potential area for further investigation would be to assess the performance of a pile with a smaller shaft diameter for the lead section, (to aid installation) and a large shaft diameter further up the pile to provide the lateral resistance that would be necessary
- An additional area for future work is to assess the impact of screw pile relative embedment depth and soil density on the geometric features investigated in this study as different installation and uplift mechanisms may affect the distribution of forces and favour different geometric properties.

4 Data Access Statement

The data presented in this paper is available online via the University of Dundee's institutional repository and may be accessed at https://doi.org/10.15132/10000169.

Acknowledgements

This research is a part of an EPSRC NPIF funded studentship with Roger Bullivant Limited. The 4th author was supported by the European Union's Horizon 2020 research and innovation programme under the Marie Skłodowska-Curie grant agreement No 753156. The authors would also like to acknowledge the further support of EPSRC (Grant no. EP/N006054/1: Supergen Wind Hub: Grand Challenges Project: Screw piles for wind energy foundations).

Accepted manuscript doi:
10.1680/jgeen.21.00104

Notation

AR	Advancement ratio
BGL	below ground level
CRP	Constant rate of penetration test
d_{100}	Maximum particle size
DEM	Discrete element method
D_h	Helix diameter
D_R	Relative density
D_s	Shaft diameter
e	Voids ratio
FEM	Finite element method
G	shear modulus
G_s	Specific gravity
H	Embedment depth
H/D_h	Relative embedment depth
K_C	Emperical torque compressive capacity correlation factor
K_T	Emperical torque tensile capacity correlation factor
N	Particle scaling factor
P_h	Helix pitch
PSD	Particle size distribution
Q_C	Compressive capacity
Q_T	Tensile capacity
R	Radius of pile helix
T	Installation torque
z	Axial displacement
γ'	Effective unit weight of soil
δ	interface friction angle
ΔD_R	change in relative density
δz	change in vertical position of particles from start to end of installation
Δz_h	Vertical displacement for one rotation
ν	Poisson's ratio
σ_{zz}	Vertical stress in soil
ϕ	critical state friction angle
μ	Friction coefficient

References

Al-Baghdadi, T. A., Brown, M. J., Knappett, J. A. and Al-Defae, A. H. (2017) 'Effects of vertical loading on lateral screw pile performance', *Geotechnical Engineering*, 170(GE3), pp. 259–272. doi: 10.1680/jgeen.16.00114.

Al-Defae, A. H. H., Caucis, K. and Knappett, J. A. A. (2013) 'Aftershocks and the whole-life seismic performance of granular slopes', *Géotechnique*. Thomas Telford Ltd, 63(14), pp. 1230–1244. doi: 10.1680/geot.12.P.149.

Arroyo, M., Butlanska, J., Gens, A., Calvetti, F. and Jamiolkowski, M. (2011) 'Cone penetration tests in a virtual chamber', *Géotechnique*, 61(6), pp. 525–531. doi: 10.1680/geot.9.P.067.

Bolton, M. D., Gui, M. W., Garnier, J., Corte, J. F., Bagge, G., Laue, J. L. and Renzil, R. (1999) 'Centrifuge cone penetration tests in sand', *Géotechnique*, 49(4), pp. 543–552. doi: 10.1680/geot.1999.49.4.543.

Butlanska, J., Arroyo, M., Gens, A. and O'Sullivan, C. (2014) 'Multiscale analysis of CPT in a virtual calibration chamber', *Canadian Geotechnical Journal*, 26(1), pp. 80–86. doi: 10.1139/cgj-2012-0476.

Cerfontaine, B., Brown, M. J., Knappett, J. A., Davidson, C., Sharif, Y. U., Huisman, M. and Ottolini, M. (2021) 'Control of screw pile installation to optimise performance for offshore energy applications', *submitted for publication to) Géotechnique*.

Ciantia, M. O. (2021) 'Micromechanics of Pile Cyclic Response in Sand', in Barla, M., Di Donna, A., and Sterpi, D. (eds) *Challenges and Innovations in Geomechanics IACMAG*. Turin, Italy: Springer, Cham, pp. 527–535. doi: 10.1007/978-3-030-64518-2_62.

Ciantia, M. O., Boschi, K., Shire, T. and Emam, S. (2018) 'Numerical techniques for fast generation of large discrete-element models', *Proceedings of the Institution of Civil Engineers - Engineering and Computational Mechanics*, 171(4), pp. 147–161. doi: 10.1680/jencm.18.00025.

Ciantia, M. O., O'Sullivan, C. and Jardine, R. (2019) 'Pile penetration in crushable soils: Insights from micromechanical modelling', in *XVII ECSMGE-2019*. Reykjavik, Iceland, pp. 298–317. doi: doi: 10.32075/17ECSMGE-2019-1111.

Das, B. M. (1990) *Earth Anchors*. 1st edn. Amsterdam Netherlands: Elsevier Science Publishers.

Davidson, C., Brown, M. J., Cerfontaine, B., Knappett, J. A., Brennan, A. J., Al-Baghdadi, T., Augarde, C., Coombs, W., Wang, L., Blake, A., Richards, D. and Ball, Jonathan, D. (2020) 'Physical modelling to demonstrate the feasibility of screw piles for offshore jacket-supported wind energy structures', *Geotechnique Published online 16/12/2020*. doi: doi.org/10.1680/jgeot.18.P.311.

Davidson, C., Brown, M.J., Brennan, A.J., Knappett, J.A., Cerfontaine, B. and Sharif, Y. U. (2019) 'Physical modelling of screw piles for offshore wind energy', in Davidson, Craig ;, Brown, Michael J., Knappett, Jonathan Adam, Brennan, Andrew J., Augarde, C. E., Coombs, W. M., Wang, L., Richards, D., White, D. J., and Blake, A. (eds)

ISSPEA. Dundee, United Kingdom: University of Dundee, pp. 31–38. doi: 10.20933/100001123.

Deeks, A. D. (2008) *An investigation into the strength and stiffness of jacked piles in sand*, *Ph. D., Cambridge University, Cambridge, U.K.* University of Cambridge, UK.

DFI (2019) *Helical Pile Foundation Design Guide*. HawThorne, New Jersey. Available at: www.dfi.org.

Elsherbiny, Z. H. and El Naggar, M. H. (2013) 'Axial compressive capacity of helical piles from field tests and numerical study', *Canadian Geotechnical Journal*, 50(12), pp. 1191–1203. doi: 10.1139/cgj-2012-0487.

Ghaly, A. and Hanna, A. (1991) 'Experimental and theoretical studies on installation torque of screw anchors', *Canadian Geotechnical Journal*, 28(3), pp. 353–364. doi: 10.1139/t91-046.

Hoyt, R. . and Clemence, S. P. (1989) 'Uplift Capacity Of Helical Anchors in Soil', in *12th International Conference on Soil Mechanics and Foundation Engineering*, pp. 1019–1022.

International Code Council (2017) *AC358 Helical Pile Systems and Devices*. Available at: https://icc-es.org/acceptance-criteria/ac358-2/.

Itasca Consulting Group, I. (2016) 'PFC 5.0'. Minneapolis: Itasca Consulting Group, Inc.

Kim, J. S., Kim, J. Y. and Lee, S. R. (1997) 'Analysis of soil nailed earth slope by discrete element method', *Computers and Geotechnics*. Elsevier, 20(1), pp. 1–14. doi: 10.1016/S0266-352X(96)00010-9.

Lauder, K. D., Brown, M. J., Bransby, M. F. and Boyes, S. (2013) 'The influence of incorporating a forecutter on the performance of offshore pipeline ploughs', *Applied Ocean Research*, 39, pp. 121–130. doi: 10.1016/j.apor.2012.11.001.

Li, Z., Haigh, S. K. and Bolton, M. D. (2010) 'Centrifuge modelling of mono-pile under cyclic lateral loads', *Physical Modelling in Geotechnics - Proceedings of the 7th International Conference on Physical Modelling in Geotechnics 2010, ICPMG 2010*, 2, pp. 965–970. doi: 10.1201/b10554-159.

Liu, J., Duan, N., Cui, L. and Zhu, N. (2019) 'DEM investigation of installation responses of jacked open-ended piles', *Acta Geotechnica*. Springer Berlin Heidelberg, pp. 1–15. doi: 10.1007/s11440-019-00817-7.

Livneh, B. and El Naggar, M. H. (2008) 'Axial testing and numerical modeling of square shaft helical piles under compressive and tensile loading', *Canadian Geotechnical Journal*, 45(8), pp. 1142–1155. doi: 10.1139/T08-044.

Lutenegger (2011) 'Historical Development of Iron Screw-Pile Foundations: 1836–1900', *The International Journal for the History of Engineering & Technology*, 81(1), pp. 108–128. doi: 10.1179/175812109x12547332391989.

Lutenegger, A. J. (2013) 'Factors Affecting Installation Torque and Torque-To-Capacity Correlations for Screw-Piles and Helical Anchors', in *Proceedings of the 1st International Geotechnical Symposium on Helical Foundations*, pp. 211–224.

McDowell, G. R., Falagush, O. and Yu, H.-S. (2012) 'A particle refinement method for simulating DEM of cone penetration testing in granular materials', *Géotechnique Letters*. Thomas Telford Ltd, 2(3), pp. 141–147. doi: 10.1680/geolett.12.00036.

Mindlin, R. D. and Deresiewicz, H. (1953) 'Elastic spheres in contact under varying oblique forces', *Journal of Applied Meechanics ASME*, 20, pp. 327–344. doi: 10.1007/978-1-4613-8865-4_35.

O'Sullivan, C., Butlanska, J. and Cheung, G. (2010) 'Calculating strain in 3D DEM simulations', *IOP Conference Series: Materials Science and Engineering*. IOP Publishing, 10, p. 12076. doi: 10.1088/1757-899x/10/1/012076.

Perko, H. A. (2009) 'Helical Piles', in *New Technological and Design Developments in Deep Foundations*. Denver: John Wiley & Sons, Inc. doi: 10.1002/9780470549063.

Richards, D., Blake, A., White, D. J., Bittar, E, M. and Lehane, B. M. (2019) 'Field Tests Assessing the Installation Performance of Screw Pile Geometries Optomised for Offshore Wind Applications', in Davidson, C. ;, Brown, M. J., Knappett, J. A., Brennan, A. J., Augarde, C. E., Coombs, W. M., Wang, L., Richards, D., White, D. J., and Blake, A. (eds) *ISSPEA*. Dundee, UK: University of Dundee, pp. 47–54. doi: 10.20933/100001123.

Robinson, S., Brennan, A. J., Knappett, J. A., Wang, K. and Bengough, G. (2019) 'Cyclic simple shear testing for assessing liquefaction mitigation by fibre reinforcement', in Silvestri, F. and Moraci, N. (eds) *Earthquake Geotechnical Engineering for Protection and Development of Environment and Constructions: Proceedings of the 7th International Conference on Earthquake Geotechnical Engineering, (ICEGE 2019)*. Rome, Italy: 1 ed. London: CRC Press, pp. 4728–4735.

Sakr, M. (2015) 'Relationship between Installation Torque and Axial Capacities of Helical Piles in Cohesionless Soils', *Journal of Performance of Constructed Facilities*, 29(6), p. 04014173. doi: 10.1061/(ASCE)CF.1943-5509.0000621.

Saleem, M. A., Malik, A. A., Ohto, T. and Kuwano, J. (2020) 'Influence of tip shape on screw pile installation effort and bearing resistance', in *The 55th Annual Meeting of the Japan National Conference on Geotechnical Engineering*.

dos Santos Filho, J. M. S. M., Morais, T. da S. O. and Tsuha, C. de H. C. (2014) 'A new experimental procedure to investigate the torque correlation factor of helical anchors', *Electronic Journal of Geotechnical Engineering*, 19 P(September 2019), pp. 3851–3864.

Schiavon, J. A., Tsuha, C., Thorel, L. and Neel, A. (2016) 'Physical modelling of cyclic loading on a single-helix anchor in sand', in *Proceedings of the 3rd European Conference on Physical Modelling in Geotechnics*. Nantes, pp. 275–279.

Sharif, Y., Brown, M. J., Ciantia, M., Knappett, J., Davidson, C., Cerfontaine, B., Robinson, S. and Ball, J. (2019a) 'Numerically Modelling the Installtion and loading of Screw Piles using DEM', in Davidson, C. ;, Brown, M. J., Knappett, J. A., Brennan, A. J., Augarde, C. E., Coombs, W. M., Wang, L., Richards, D., White, D. J., and Blake, A. (eds) *International Symposium on Screw Piles for Energy Applications*. Dundee, UK: University of Dundee, pp. 101–108. doi: 10.20933/100001123.

Sharif, Y., Ciantia, M., Brown, M. J., Knappett, J. A. and Ball, J. D. (2019b) 'Numerical Techniques For the Fast Generation of Samples Using the Particle Refinement Method', in *Proceedings of the 8th International Conference on Discrete Element Methods*. Enschede, Netherlands, p. 181.

Sharif, Y. U., Brown, M. J., Cerfontaine, B., Davidson, C., Ciantia, M. O., Knappett, J., Ball, J. D., Brennan, A. J., Augarde, C. E., Coombs, W., Blake, A., Richards, D., White, D., Huisman, M. and Ottolini, M. (2020b) 'Effects of screw pile installation on installation requirements and in-service performance using the Discrete Element Method', *Canadian Geotechnical Journal*. Canadian Science Publishing. doi: 10.1139/cgj-2020-0241.

Sharif, Y. U., Brown, M. J., Ciantia, M. O., Cerfontaine, B., Davidson, C., Knappett, J., Meijer, G. J. and Ball, J. (2020a) 'Using DEM to create a CPT based method to estimate the installation requirements of rotary installed piles in sand', *Canadian Geotechnical Journal published online 19/08/2020*. doi: http://dx.doi.org/10.1139/cgj-2020-0017.

Shi, D., Yang, Y., Deng, Y. and Xue, J. (2019) 'DEM modelling of screw pile penetration in loose granular assemblies considering the effect of drilling velocity ratio', *Granular Matter*. Springer Berlin Heidelberg, 21(3), pp. 1–16. doi: 10.1007/s10035-019-0933-3.

Tovar-Valencia, R. D., Galvis-Castro, A., Salgado, R. and Prezzi, M. (2021) 'Effect of Base Geometry on the Resistance of Model Piles in Sand', *Journal of Geotechnical and Geoenvironmental Engineering*. American Society of Civil Engineers (ASCE), 147(3), p. 04020180. doi: 10.1061/(asce)gt.1943-5606.0002472.

Tsuha, C. de H. C. and Aoki, N. (2010) 'Relationship between installation torque and uplift capacity of deep helical piles in sand', *Canadian Geotechnical Journal*, 47(6), pp. 635–647. doi: 10.1139/T09-128.

Urabe, K., Tokimatsu, K., Suzuki, H. and Asaka, Y. (2015) 'Bearing Capacity and Pull-Out Resistance of Wing Piles During Cyclic Vertical Loading', in *Proceedings of the 6th International Conference on earthquake Geotechnical Engineering*. Christchurch, new Zealand, pp. 358–367.

Table 1: HST95 sand physical and numerical properties (Sharif *et al.* 2019a)

HST95 silica sand property	Value
Physical properties	
Sand unit weight γ (kN/m^3)	16.75
Minimum dry density γ_{max} (kN/m^3)	14.59
Maximum dry density γ_{min} (kN/m^3)	17.58
Critical state friction angle, φ (degrees)	32
Interface friction angle, δ (degrees)	18
Specific gravity, G_s	2.65
D_{30} (mm)	0.12
D_{60} (mm)	0.14
DEM Parameters	

Shear modulus, G (GPa)	3
Friction coefficient, μ (-)	0.264
Poisson's ratio, ν (-)	0.3
Interface friction coefficient [pile], μ_{pile} (-)	0.16

Table 2: Properties of soil bed used in this study

Property	Dense
Relative Density (%)	84
Voids ratio (e)	0.52
Height (m)	32
Radius (m)	20
Core PSD scaling (N_c)	20
Number of Particles	270,000

Table 3: List of model pile dimensions, advancement ratio (AR), helix diameter (D_h), helix pitch (P_h), base geometry and shaft diameter (D_h) of all simulations conducted in this study

Simulation ID	Pile ID	AR [-]	D_h (m)	D_s (m)	P_h (m)	Base geometry	D_h/D_s (-)	P_h/D_h (-)
1	1	1	1.7	0.88	0.56	Flat	1.93	0.33
2	2	1	1.7	0.88	0.56	Conical	1.93	0.33
3	3	1	1.7	0.88	0.56	Asymmetric cut off	1.93	0.33
4	4	1	1.7	0.88	1.2	Flat	1.93	0.71
5	5	1	1.7	0.6	0.56	Flat	2.83	0.33
6	6	1	1.7	1.2	0.56	Flat	1.42	0.33
7	1	0.5	1.7	0.88	0.56	Flat	1.93	0.33
8	2	0.5	1.7	0.88	0.56	Conical	1.93	0.33
9	3	0.5	1.7	0.88	0.56	Asymmetric cut off	1.93	0.33
10	4	0.5	1.7	0.88	1.2	Flat	1.93	0.71
11	5	0.5	1.7	0.6	0.56	Flat	2.83	0.33
12	6	0.5	1.7	1.2	0.56	Flat	1.42	0.33

Table 4: Summary of pile total installation torque, axial capacities and back-calculated torque capacity correlation factors for all pile geometries and advancement ratios

Pile ID	Advancement ratio (AR) [-]	Total Installation Torque (T) [MNm]	Tensile capacity (Q_T) [MN]	Compressive capacity (Q_C)[MN]	Tensile Torque factor (K_t)[m^{-1}]	Compressive Torque factor (K_c)[m^{-1}]	Q_T/Q_C
1	1	5.48	6.27	31.07	1.14	5.67	0.20
2	1	5.24	5.99	27.14	1.14	5.18	0.22

3	1	6.4	6.63	25.86	1.04	4.04	0.26
4	1	4.54	8.82	18.29	1.94	4.03	0.48
5	1	4	5.2	28.57	1.30	7.14	0.18
6	1	5.94	11.3	28.64	1.90	4.82	0.39
1	0.5	5.58	10.4	16.79	1.86	3.01	0.62
2	0.5	5.5	11.37	12.21	2.07	2.22	0.93
3	0.5	6.4	11.49	14.01	1.80	2.19	0.82
4	0.5	4.71	11.95	21.29	2.54	4.52	0.56
5	0.5	3.6	8.06	17.86	2.24	4.96	0.45
6	0.5	5.97	13.7	17.57	2.29	2.94	0.78

Table 5: Summary of pile total installation torque, axial capacities and back-calculated torque capacity correlation factors for all pile geometries and advancement ratios

Pile ID	Advancement ratio (AR) [-]	Total Installation Torque (T) [MNm]	Tensile capacity (Q_T) [MN]	Compressive capacity (Q_C)[MN]	Tensile Torque factor (K_t)[m^{-1}]	Compressive Torque factor (K_c)[m^{-1}]	Q_T/Q_C
1	1	5.48	6.27	31.07	1.14	5.67	0.20
2	1	5.24	5.99	27.14	1.14	5.18	0.22
3	1	6.4	6.63	25.86	1.04	4.04	0.26
4	1	4.54	8.82	18.29	1.94	4.03	0.4

							8
5	1	4	5.2	28.57	1.30	7.14	0.18
6	1	5.94	11.3	28.64	1.90	4.82	0.39
1	0.5	5.58	10.4	16.79	1.86	3.01	0.62
2	0.5	5.5	11.37	12.21	2.07	2.22	0.93
3	0.5	6.4	11.49	14.01	1.80	2.19	0.82
4	0.5	4.71	11.95	21.29	2.54	4.52	0.56
5	0.5	3.6	8.06	17.86	2.24	4.96	0.45
6	0.5	5.97	13.7	17.57	2.29	2.94	0.78

Figure captions

Figure 1: Schematic diagram of the geometry of all piles used within this study.

Figure 2: Example cross section through the model soil bed used in DEM simulations, shading indicates the particle size distribution scaling applied, prototype diameter 40.0m, prototype height 32.0m and D_R = 84%.

Figure 3: Total installation requirements with depth for all screw pile geometries investigated in this study a) Total installation force (*AR* = 1.0) b) Total installation torque (*AR* = 1.0) c) Total installation force (*AR* = 0.5) d) Total installation torque (*AR* = 0.5)

Figure 4: Comparison of installation requirements with depth and axial capacity tests for base case pile (U1VDB) a) Compressive installation force b) Installation torque c) Compression CRP d) Tension CRP

Figure 5: Base component of installation requirements for screw pile with different base geometries installed at *AR* = 1.0 and 0.5 a) Installation force b) Installation torque

Figure 6: In-service axial resistance of screw piles with varying base geometries installed at *AR* = 1.0 and 0.5 a) compressive resistance b) tensile resistance

Figure 7: Helix component of installation requirements for screw piles with P_h = 0.56m and 1.20m installation at an *AR* = 1.0 and 0.5. a) Installation force b) Installation torque

Figure 8: In-service axial resistance of screw piles with varying helix pitch installed at *AR* = 1.0 and 0.5. a) Compressive resistance b) Tensile resistance

Figure 9: Comparison of soil state post installation for screw piles with varying shaft diameters installed under pitch-matched conditions a) Residual vertical stress at the end of installation produced by screw piles with different helix pitches installed at AR = 1.0 b) Comparison of particle vertical displacement during installation for piles with different helix pitches installed at AR = 1.0

Figure 10: In-service axial resistance of screw piles with varying shaft diameters installed at AR = 1.0 and 0.5. a) Compressive resistance b) Tensile resistance

Figure 11: Comparison of soil state post installation for screw piles with varying shaft diameters installed under pitch-matched conditions a) change in relative density from beginning to end of installation b) residual locked in vertical stress at the end of installation.

Accepted manuscript doi:
10.1680/jgeen.21.00104

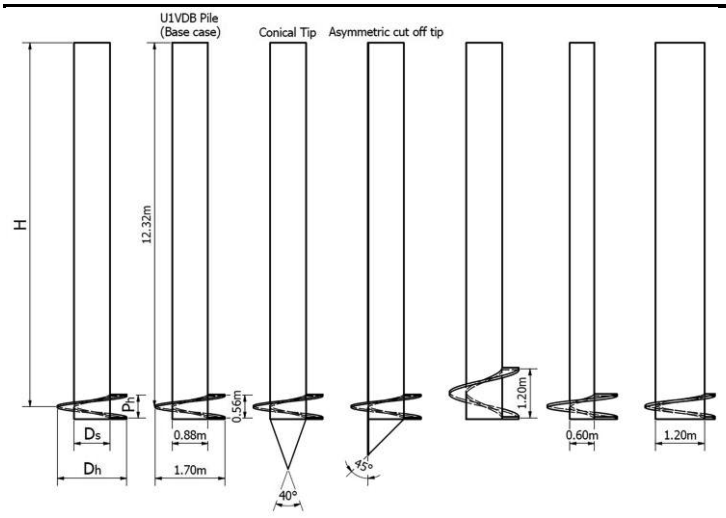

Figure 1

Accepted manuscript doi:
10.1680/jgeen.21.00104

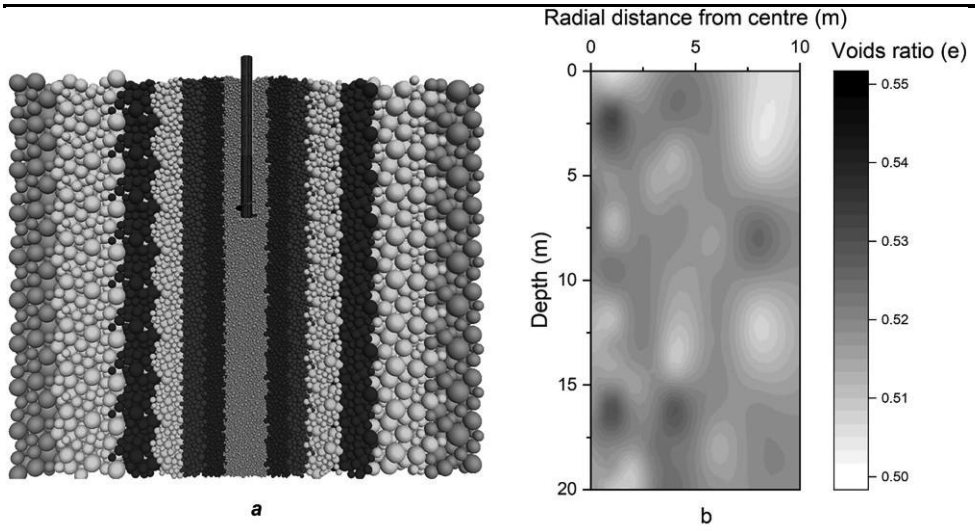

Figure 2

Accepted manuscript doi:
10.1680/jgeen.21.00104

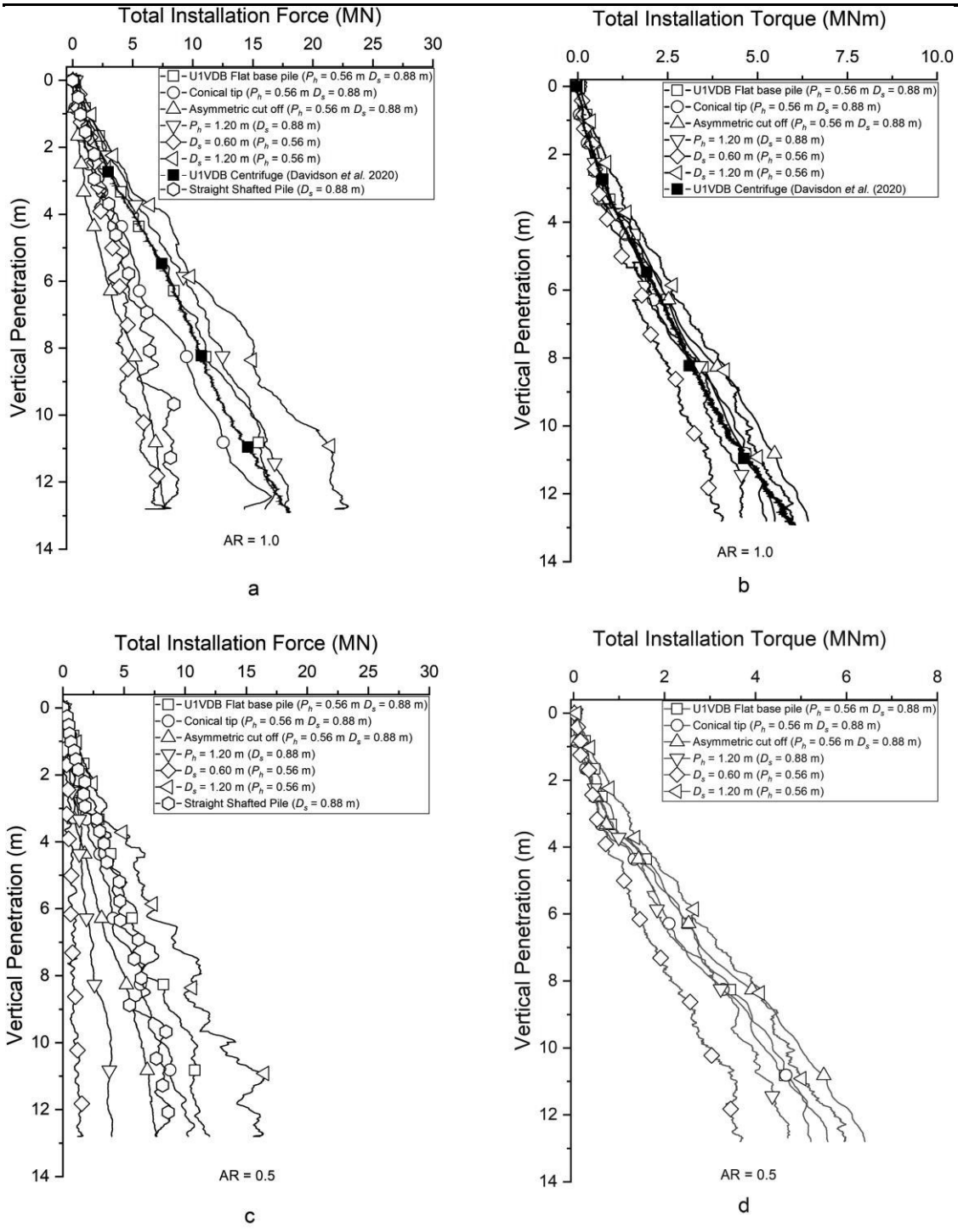

Figure 3

Accepted manuscript doi:
10.1680/jgeen.21.00104

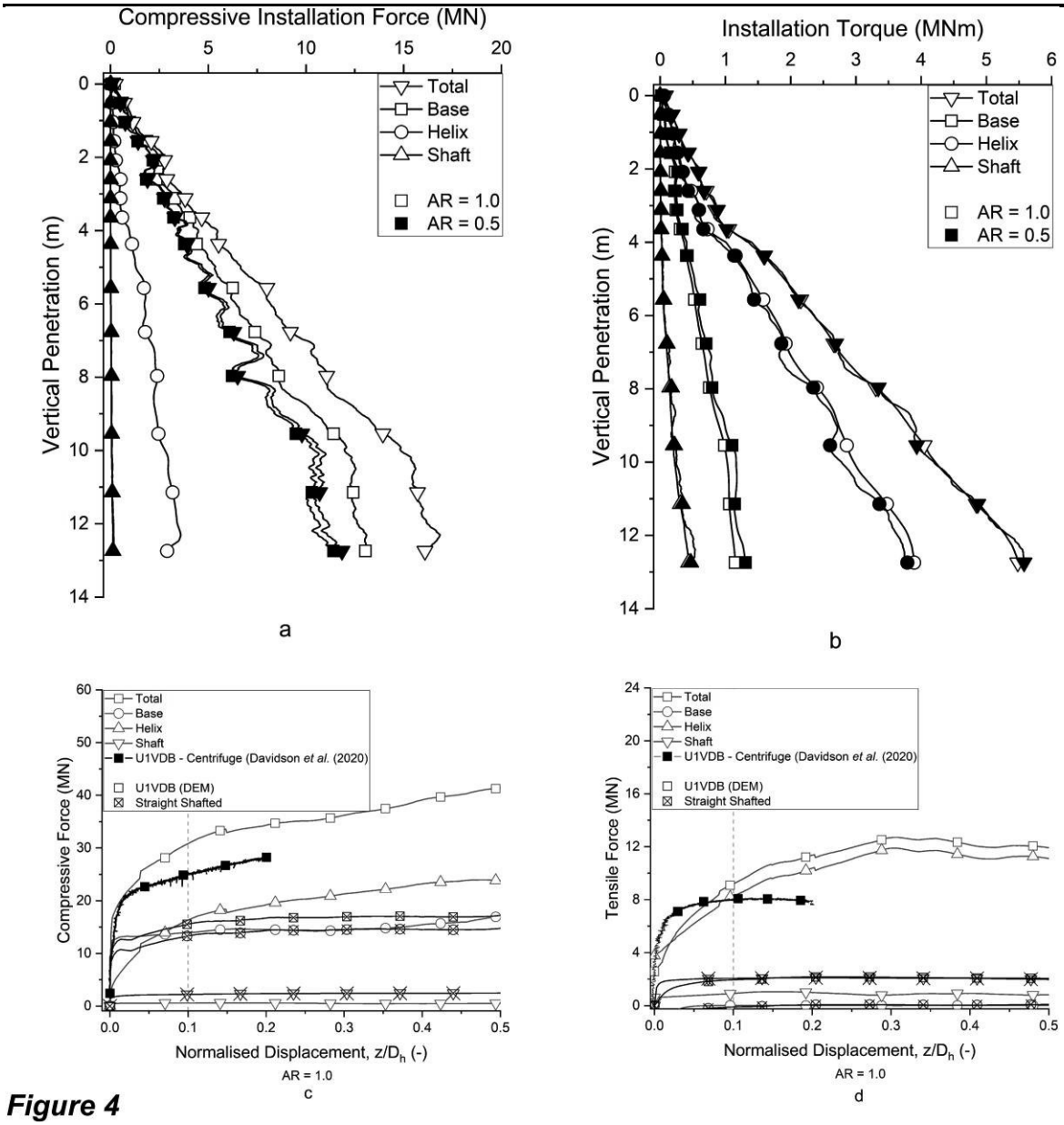

Figure 4

Accepted manuscript doi:
10.1680/jgeen.21.00104

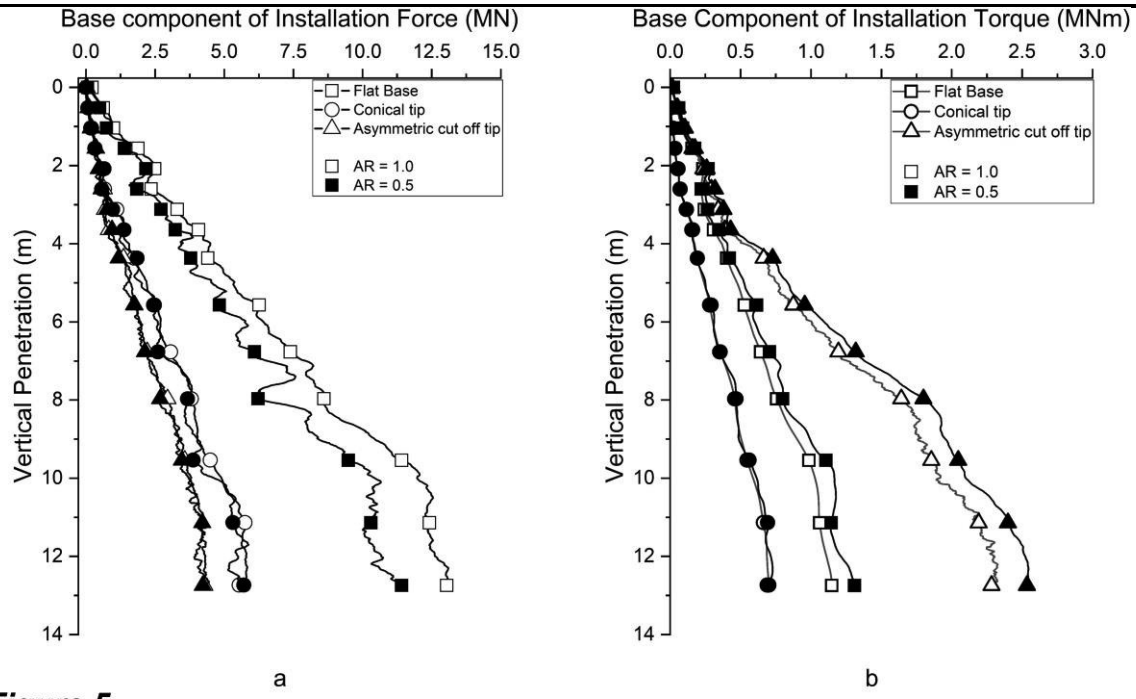

Figure 5

Accepted manuscript doi:
10.1680/jgeen.21.00104

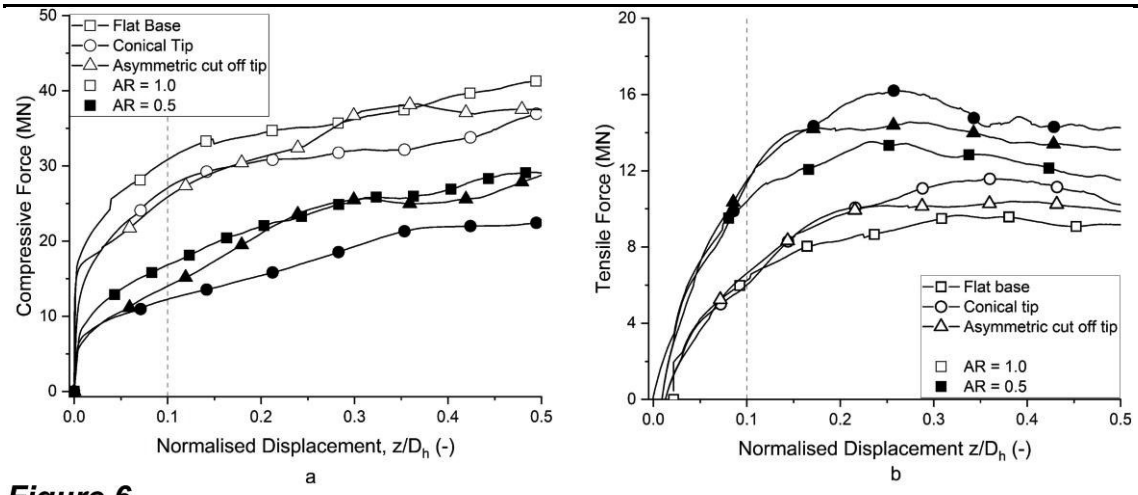

Figure 6

Accepted manuscript doi:
10.1680/jgeen.21.00104

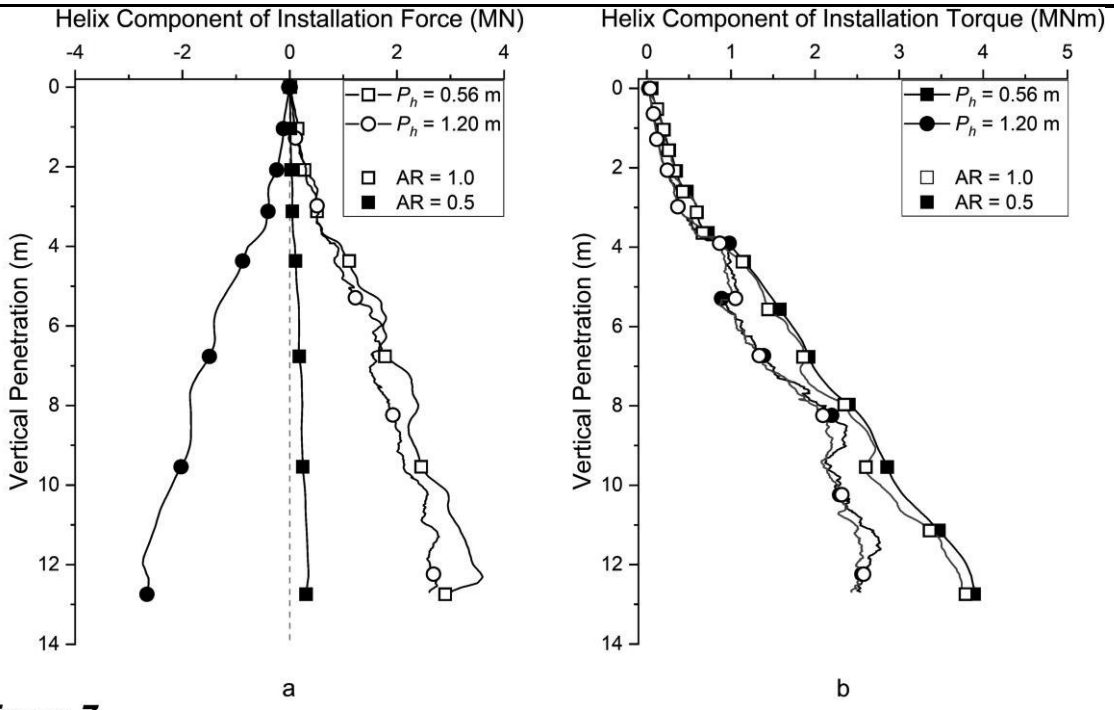

Figure 7

Accepted manuscript doi:
10.1680/jgeen.21.00104

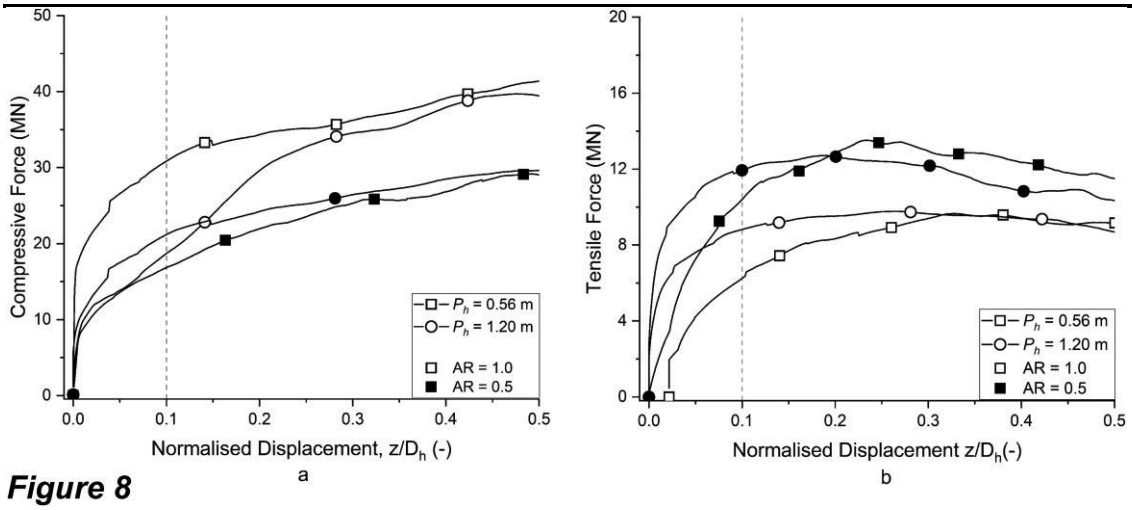

Figure 8

Accepted manuscript doi:
10.1680/jgeen.21.00104

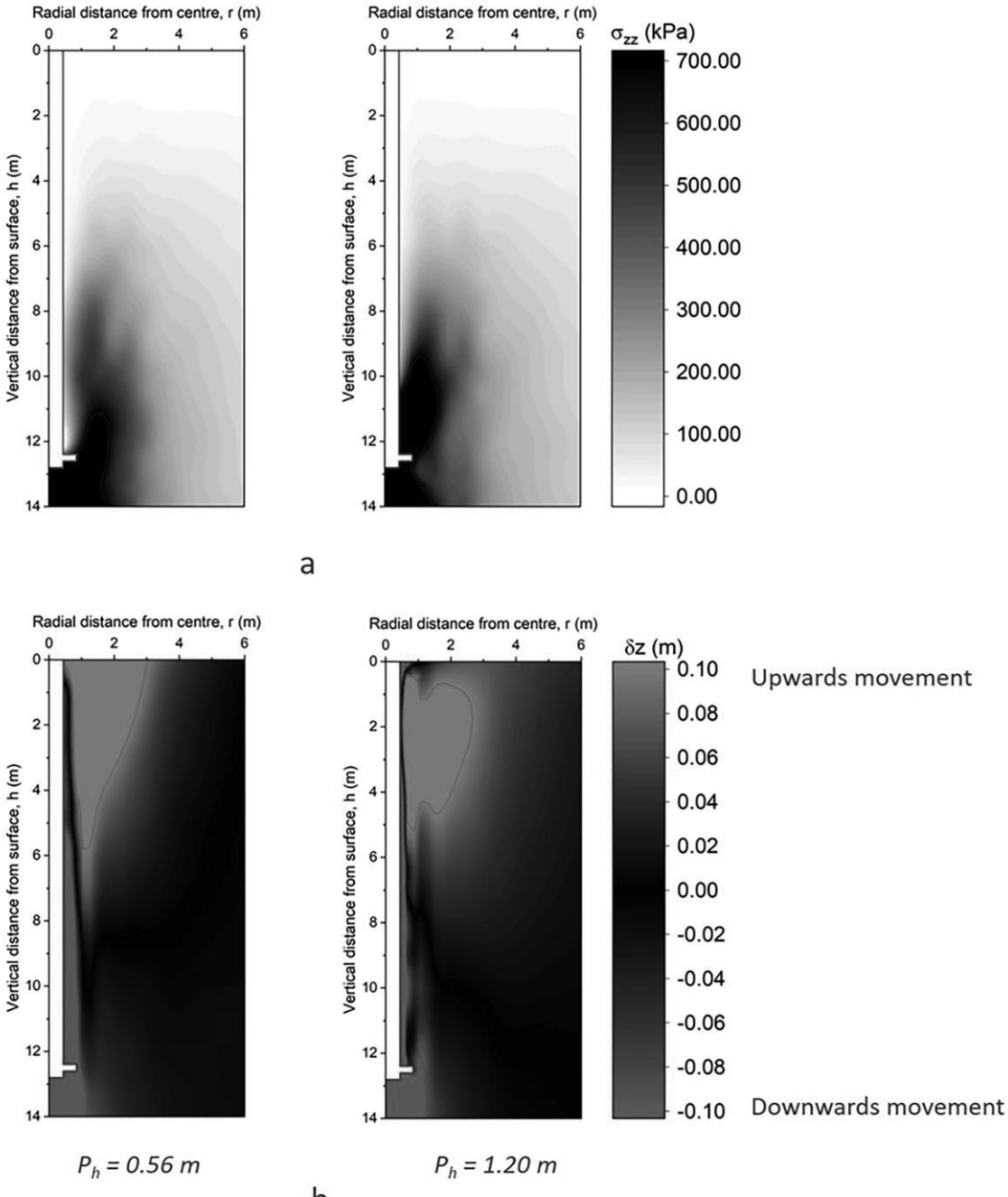

Figure 9

Accepted manuscript doi:
10.1680/jgeen.21.00104

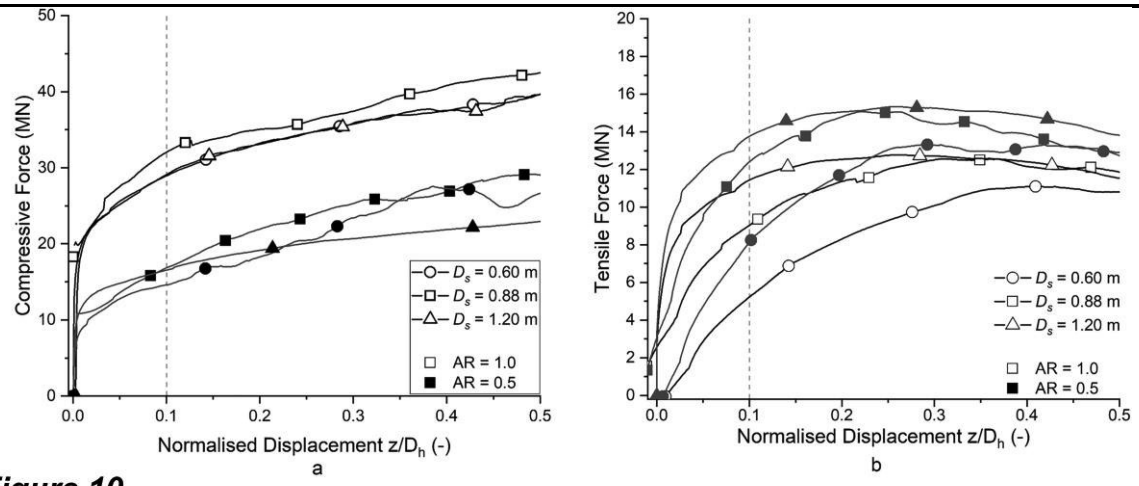

Figure 10

Accepted manuscript doi:
10.1680/jgeen.21.00104

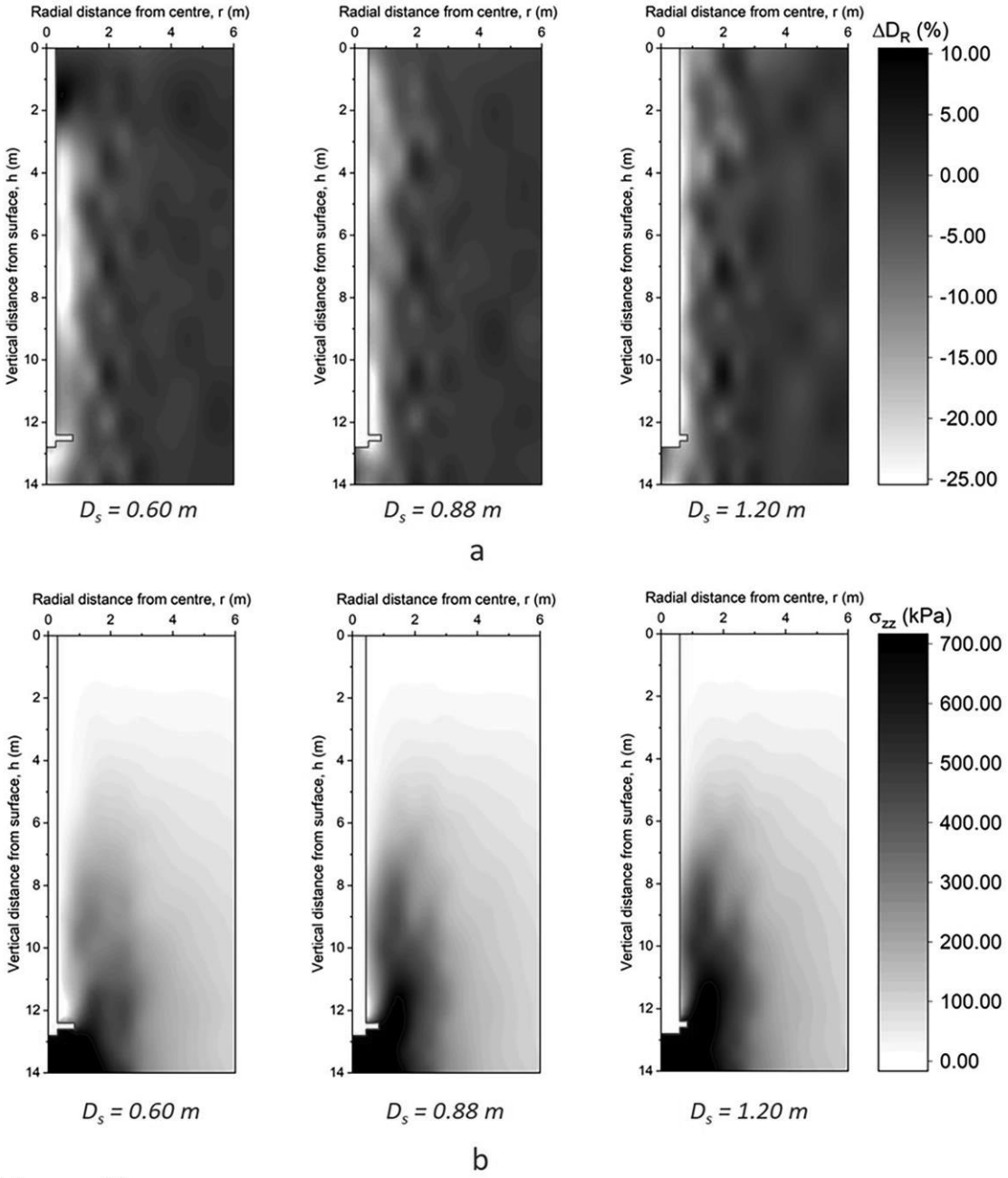

Figure 11